Velocity Fields of Distant Galaxies with FORS2

Bodo Ziegler[1]
Elif Kutdemir[2]
Cristiano Da Rocha[1]
Asmus Böhm[3]
Wolfgang Kapferer[3]
Harald Kuntschner[1]
Reynier Peletier[2]
Sabine Schindler[3]
Miguel Verdugo[4]

[1] ESO
[2] Kapteyn Institute, Groningen, the Netherlands
[3] University of Innsbruck, Austria
[4] University of Göttingen, Germany

We describe a method of obtaining two-dimensional velocity fields of distant, faint and small, emission-line galaxies efficiently with FORS2 at the VLT. The fields are examined for kinematic substructure to identify possible interaction processes. Numerical simulations of tidal interactions and ram pressure effects reveal distinct signatures observable with our method. We detect a significant fraction of galaxies with irregular velocity fields both in the field and cluster environments.

Galaxy formation and evolution are still principal research topics in modern astrophysics, and have been investigated since objects outside the Milky Way were recognised after the Great Debate between Shapley and Curtis. The main questions include: When and how did galaxies form? Why are there different morphological types? What is the role of environment? The models used to answer these questions range from single epoch to continous creation scenarios. The current theoretical paradigm of a cold dark matter (CDM) dominated Universe predicts a hierarchical bottom-up structure evolution from small entities towards bigger systems through merging. During such a process spiral galaxies can be transformed into ellipticals. However, the disc component can be regained through subsequent new gas accretion and star formation. Many irregular and peculiar galaxies are observed in clusters of galaxies, in which they may experience interactions in addition to merging and accretion.

Much progress has been achieved in recent years by deep photometric surveys (like GOODS) finding galaxies and quasars at high redshift ($z \sim 6$) corresponding to an epoch just a billion years after the Big Bang. These surveys have revealed a dichotomy between blue, star-forming and red, passive galaxies at later times, with an evolutionary transition between the two groups. Spectroscopic surveys (like CFHRS) have additionally produced evidence that there is a sharp decline in the overall star formation activity in the cosmos within the last eight billion years. However, all these results are based on measurements of the luminosity as produced by the stars, while the total mass of a galaxy is mainly composed of dark matter. Because the triggering and process of star formation contains complicated physics, we need to make many assumptions and simplifications in our modelling, and, in addition, we do not clearly understand the scaling between the baryonic and dark matter. Therefore, it would be more favourable if we could determine observationally the total mass of galaxies and compare its evolution directly to the predicted structure assembly.

Such measurements of the dynamical mass of even faint and small, very distant galaxies were achieved recently by a number of research groups using the largest telescopes. Through spectroscopy they derive the internal kinematics (motions) of the stellar systems that are subject to the whole gravitational potential. In the optical wavelength regime, we can conduct these measurements out to redshifts of one. For spiral galaxies, we can determine the rotation curve from gas emission lines (like [O II] at 372.7 nm restframe wavelength). If the galaxy is undisturbed, the rotation curve rises in the inner part and turns over into a flat plateau dominated by its dark halo and we can calculate the maximum rotation velocity V_{max}. In such a case the assumption of virialisation holds, so that we can use the Tully–Fisher relation TFR (Tully & Fisher, 1977) as a powerful diagnostic tool that scales the baryonic matter (parameterised, e.g., by stellar luminosity) to the dark matter (as given by V_{max}). Our group, for example, has found that the TFR of 130 distant ($z = 0.5$, on average) field galaxies has a shallower slope than the local one if restframe *B*-band luminos-ities are considered, so that the brightening of a slow rotator is much larger than that of a fast rotator (Böhm & Ziegler, 2007). This result can be interpreted principally in two ways: either the majority of distant galaxies are much more scattered around the TFR and we do not see enough regular spirals at the faint end; or, there is a mass-dependent evolution with low-mass objects exhibiting on average a stronger effect over the last five billion years. The latter scenario is supported by modelling the chemical evolution of our galaxies that has revealed less efficient, but extended, star formation for slow rotators (Ferreras et al., 2004) and is consistent with other observational evidence for a mass-dependent evolution (often called ”downsizing’’).

For a correct application of the TF analysis a galaxy must be undisturbed, so that the assumption of virial equilibrium is fulfilled and, therefore, the rotation curve shows a very regular shape. If this is not the case, can we then still learn something? In the CDM structure formation theory, galaxies evolve by merging and accretion, so that we can look for kinematic signatures of such events and whether there is an increase in the abundance of such types with redshift. To investigate a possible environmental dependence, we need to disentangle such collisions from the numerous other interaction phenomena that galaxies can experience in groups and clusters.
The gas content of spirals reacts to the ram pressure exerted by the intracluster medium, a hot plasma permeating the whole structure. Part of the gas can also be stripped off by tidal forces (sometimes called “strangulation”). Other processes like harassment can even remove stars from galaxy discs, so that the overall morphology is altered. However, (irregular) rotation curves from slit spectroscopy do not contain unique information to reveal a specific interaction process unambigously. In addition, peculiar shapes can sometimes be caused artificially by observational and instrumental effects when long slits are used (Ziegler et al., 2003; Jäger et al., 2004). A more favourable observation would, therefore, be that of a two-dimensional velocity field.

FORS2 spectroscopy to obtain velocity fields

Many large telescopes today offer 3D-spectroscopy and most future facilities (like the European Extremely Large Telescope) will provide such instrument modes. At the VLT, for example, VIMOS and FLAMES offer integral field unit (IFU) spectroscopy in the optical regime. For our specific purpose, however, we conceived a different method of obtaining velocity fields that has many advantages for our science case: matched galaxy sizes, good spatial resolution, long wavelength range and high efficiency through a large number of simultaneous targets and economic exposure times (see Kutdemir et al., 2008).

For our procedure, we utilise the MXU mode of FORS2 that allows slits to be cut individually and at any desired orientation into a mask by a laser. We pick up a particular target and start with a slit placed along the photometric major axis, as measured on spatially highly resolved images from the Hubble Space Telescope/Advanced Camera for Surveys (HST/ACS; Figure 1). The slit covers the full size of the galaxy in its mid-plane with width 1 arcsecond and extends much beyond it to allow an accurate sky subtraction (common slit lengths are 15–25 arcseconds). In the same manner, 20–30 more slits are placed on other targets across the full field of view of FORS2 (6.8 × 6.8 arcminutes), with, occasionally, even two or three objects falling into the same slit. Observations with such a mask will eventually yield rotation curves, as for our previous projects, with one spatial axis and one velocity axis by measuring the centre positions of an emission line row-by-row along the spatial profile of the two-dimensional galaxy spectrum (Böhm et al., 2004). In order to construct a velocity field with two spatial axes, we observe all targets twice more with different slit positions using two more masks. This time slits are offset by 1 arcsecond along the minor axis of the galaxy to either side of the first position, so that all three slit positions together correspond to a rectangular grid (Figure 1). In that way, the full extent of a galaxy is covered, which is particularly important for a TF (viz. undisturbed) galaxy, where we need to measure the flat part of the rotation curve, which is usually reached at about three disc scale lengths. At the redshifts of our targets (z = 0.1–1.0), this corresponds to angular sizes of about 3–6 arcseconds. The spatial resolution along the x-axis of our grid is given by the pixel size of the FORS2 CCD chips of 0.25 arcseconds. For the y-axis, we are restricted by the slit width of 1.0 arcsecond, which is a good compromise between minor loss of light falling out of the slit due to seeing, adequate spectral resolution (R = 1000), and spatial sampling in the y-direction.

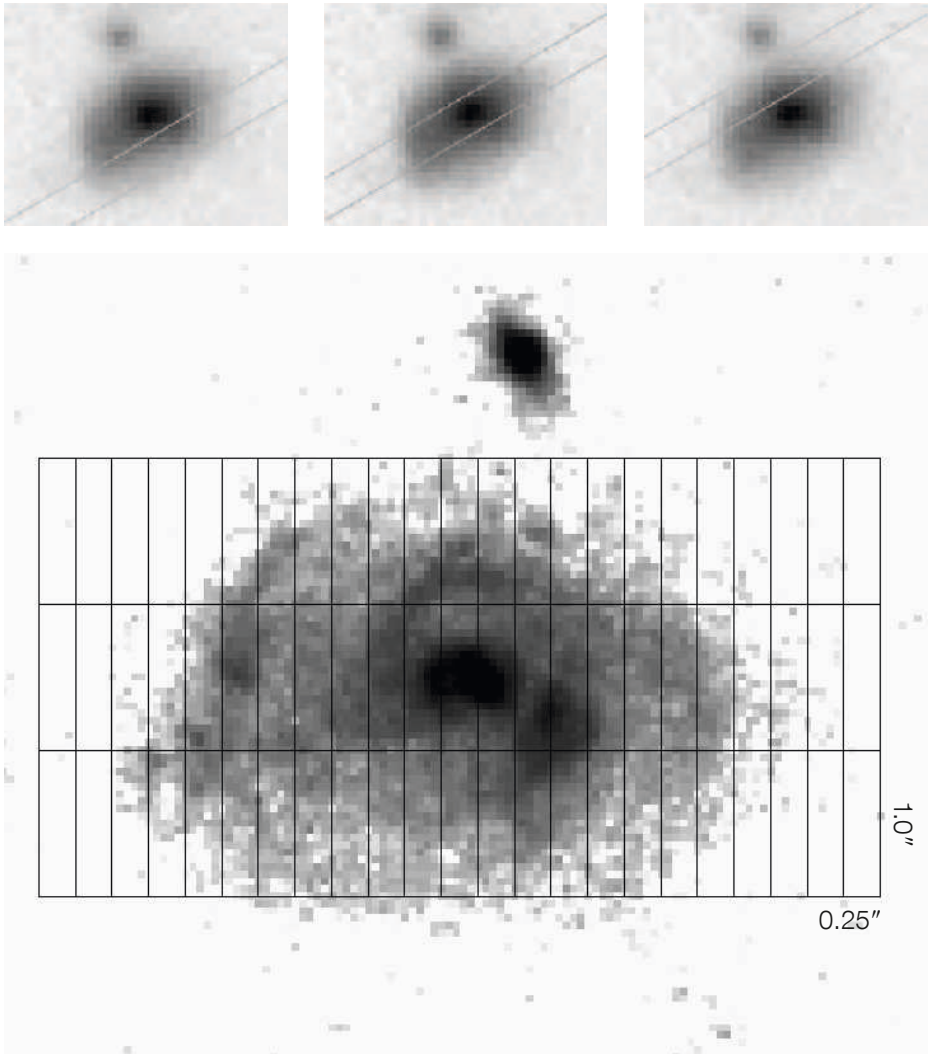

Figure 1. Our method for obtaining two-dimensional velocity fields with FORS2 is based on the observation of three different slit positions per target (upper). The combination of the measurements yields independent data points for a rectangular grid covering the whole galaxy (lower). From Kutdemir at al., 2008.

For the spectral element we use a high-throughput holographic VPH grism (600RI) that results in a long wavelength range (330 nm) projected onto the CCD. This has two advantages: for each galaxy several gas emission lines and many absorption lines of the stellar continuum are visible; then both sets of lines can be combined to derive the stellar rotation curve in addition to the gaseous one. Depending on the redshift of the object, emission lines from the blue [OII] line (at 372.7 nm) to the red Hα line (at 656.3 nm) are visible. While up to seven different lines can be observed in case of some field galaxies, most cluster members have four (Figure 2). This allows us to derive rotation curves and velocity fields in several independent ways and to check for consistency. In addition it also allows us to investigate possible depend-

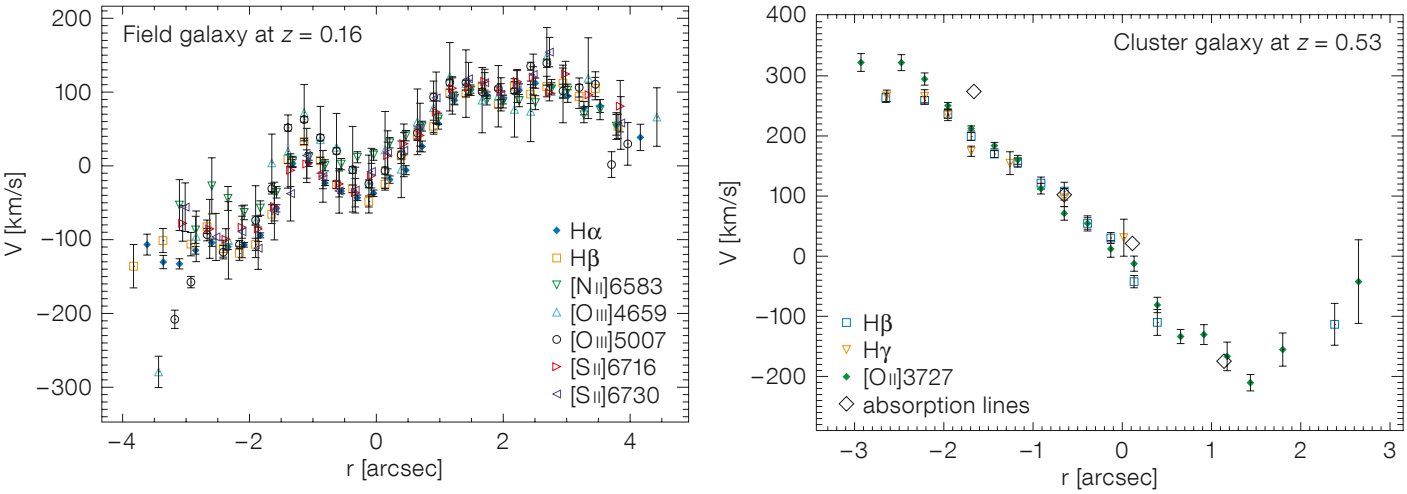

Figure 2. Two examples of rotation curves derived from the central slit. For some field galaxies up to seven different emission lines can be used independently to study the *gas* kinematics across a galaxy (left). For brighter galaxies, even *stellar* rotation curves can be measured by combining many absorption lines (right). From Kutdemir at al., 2008.

encies on the physical state of the gas clouds that emit the respective lines (all galaxies have both recombination and forbidden emission lines). From line ratios, we can then construct metallicity maps and assess a possible contribution from active galactic nuclei (AGN) activity in addition to star formation.

Despite the need for the observation with three masks in order to construct a velocity field, our method is still highly efficient. The VPH grism with its medium spectral resolution, together with the excellent optics of FORS2 mean that sufficient signal can be reached in an emission line to measure the line centres in each spectral (CCD) row accurately with 2.5 hours total integration time. This holds also for the outer regions of the galaxies, where the surface brightness drops to low values (from typically 22 V_{mag}/sq. arcsecond in the inner part to about 26 V_{mag}/sq. arcsecond). Therefore, we can obtain the necessary data for a large number of objects (20–30) within a total integration time of only 7.5 hours. For comparison, FLAMES observations with 15 IFUs of similar targets need integration times of 8–13 hours.

The standard reduction of the spectroscopic images produces a wavelength calibrated two-dimensional spectrum for each slit position of the mask separately. Thanks to the high stability of FORS, exposures of the same mask taken on different nights can be combined into a single deep spectrum. As for the determination of rotation curves, the wavelength of the centre position of a given emission line is measured along the spatial profile. Differences from a common systemic centre can then be translated into velocity space, applying Doppler's rule. The construction of the velocity field, VF, needs a very careful combination of the measurements from the three slit positions. So that we knew the exact position of the masks relative to each other, we also included a few stars with narrow slits perpendicular to each other. These stellar spectra are also used to determine the seeing during the exposure. In addition, for a third of the galaxies per mask the central slit position was taken, while the other two thirds had the off-centre positions, thus alleviating both mask acquisition during observations and mask combination in data reduction. To set up the VF, each position–velocity data point is then calcu-

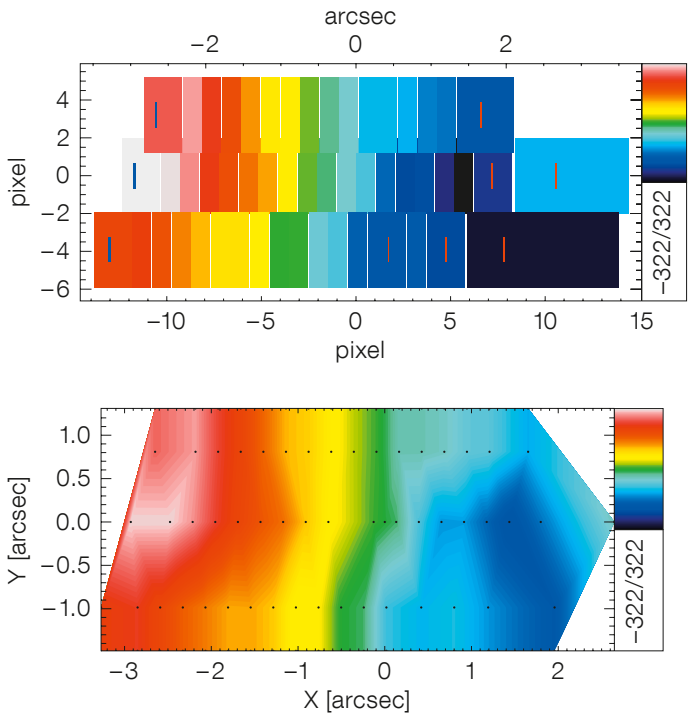

Figure 3. Example of an observed velocity field of a cluster spiral at z = 0.5 displayed in the upper panel as binned independent data points and in the lower panel linearily interpolated for visualisation purposes (from Kutdemir at al., 2008).

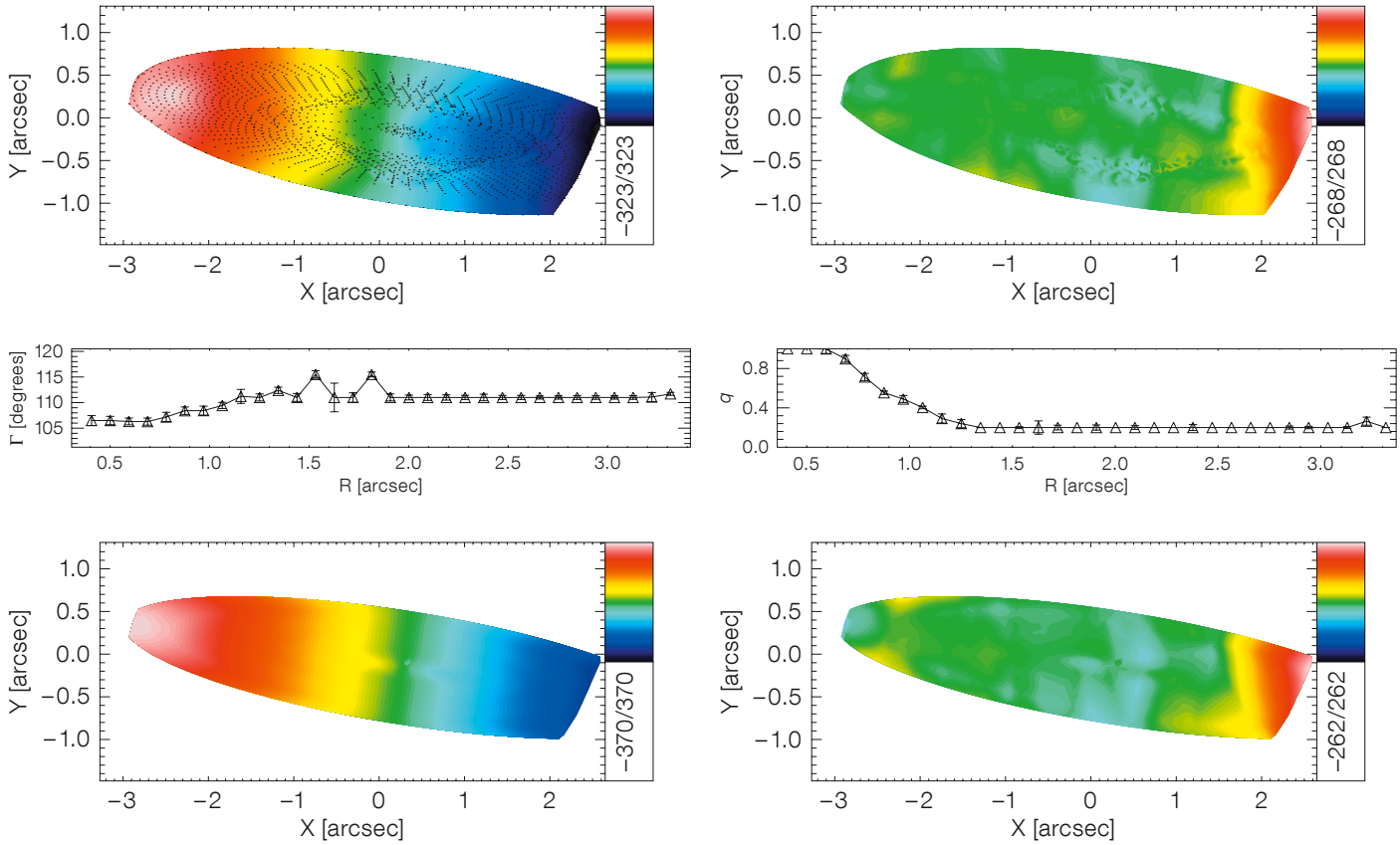

Figure 4. Velocity field of the galaxy in Figure 3 reconstructed by kinemetry with best-fitting ellipses overplotted (top left) and its residual map (top right) obtained by subtracting the model from the observed field. A model (bottom left) and its residual (bottom right) of the circular velocity component (rotation map) constructed for the average value of the kinematic position angle Γ and flattening q (shown in the middle panels as function of distance to the kinematic centre) (from Kutdemir at al., 2008).

lated within a common coordinate system, whose origin was determined from the intensity maximum of the spatial profile around the emission line in the central slit and its respective wavelength. An example is shown in Figure 3.

Kinemetric analysis of velocity fields

Since our VFs cover a large fraction of a galaxy's extent with good spatial resolution, we can analyse them quantitatively in some detail. We use kinemetry (Krajnovic et al., 2006), originally developed for nearby galaxies observed with the SAURON 3D-spectrograph, whose VFs have much higher signal and resolve much smaller physical scales than is the case of our distant targets. In polar coordinates the velocity profile of a flat rotating disc can be described by a cosine function of the azimuthal angle. Best-fitting ellipses, along which the velocity profiles are extracted, can be determined as a function of radius. Deviations from these fits can be quantified by a harmonic Fourier expansion, whose coefficients can be interpreted in terms of physical parameters. While the first order reflects the bulk motion (the rotation), the third and fifth orders, for example, describe the correction to simple rotation and indicate separate kinematic components. For the reconstruction of the intrinsic velocity map, the free parameters are the flattening and the position angle of the ellipses, while their centres are fixed to a common origin. An example of a reconstructed velocity map with best-fitting ellipses overplotted is given in Figure 4. When, instead, the inclination and position angle are fixed to their average global value, a simple rotation field along the kinematic major axis can be modelled. Its residuals with respect to the observed VF may indicate non-circular velocity components like streaming motions along spiral arms or along a bar. Additional components such as a decoupled core can be recognised in such a residual map, too, not only from an increase in the k_5 Fourier coefficient, but also by twists in the position angle and flattening. A rotation curve is extracted from the observed VF along the kinematic major axis to determine V_{max} accurately, which may be different from the one derived from the curve along the central slit aligned with the photometric axis.

Simulations of interactions: structure and kinematics

One of the main goals of our project is to identify signatures of possible interaction events. Galaxies may be transformed from one type into another not only by merging or accretion, but also by other effects like ram-pressure stripping or harassment in the environment of a cluster or group. Open questions are still: which processes are efficient under what conditions and whether there is a dominant

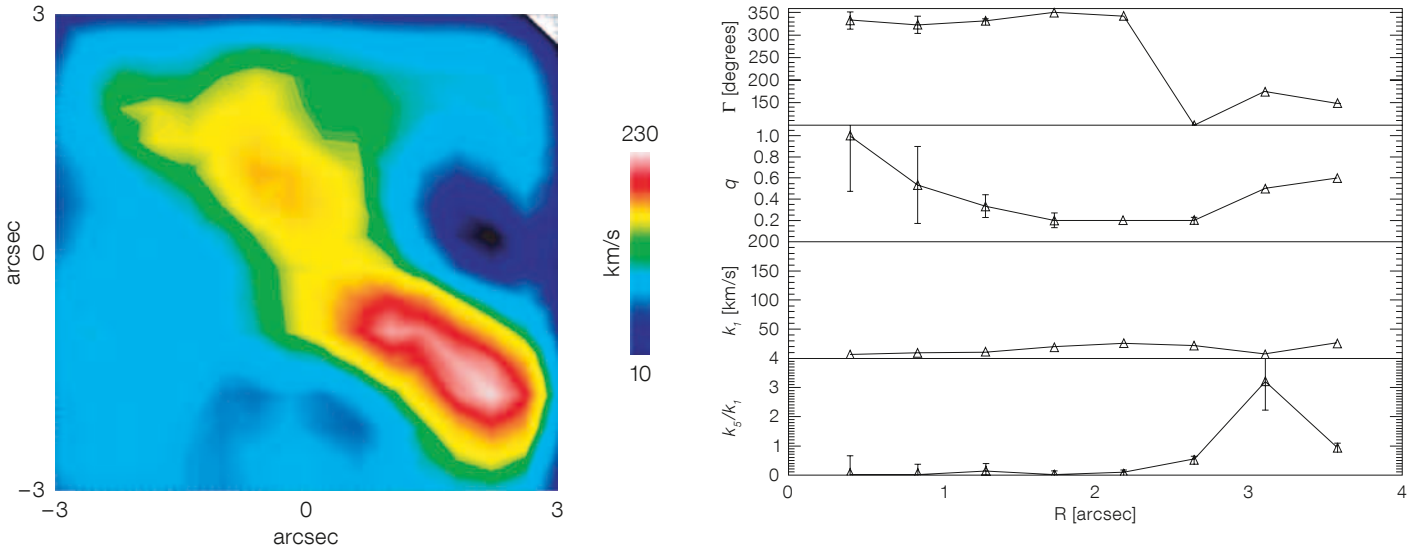

Figure 5. Velocity field of a simulated major merger as would be observed at $z = 0.1$ (left) and radial profiles of some parameters (kinematic position angle, flattening, first Fourier coefficient indicating the bulk motion and normalised fifth Fourier coefficient indicating separate kinematic components) determined by kinemetry (right). The case shown refers to a small galaxy that has penetrated a bigger one, seen 200 Myr after the event (from Kronberger at al., 2007).

mechanism responsible for the abundance of elliptical galaxies in local rich clusters. In order to study systematically the distortions and irregularities in rotation curves and velocity fields caused by interaction phenomena, we performed N-body/soft particle hydrodynamics (SPH) simulations and extracted both structural and kinematic information from the computer output in the same manner as from observational data. The numerical calculations were carried out for the three components — dark matter halo, stellar body and collisional gas clouds — of a galaxy and are based on the Gadget2 code (Springel, 2005) that incorporates hydrodynamic physics (and has explicit prescriptions for star formation and feedback).

So far, we have modelled minor mergers, major mergers, tidal interactions caused by fly-bys and ram-pressure stripping (Kronberger et al., 2007; 2008). There are large variations in the degree of distortions both in stellar structure and gas kinematics in the case of the first three of these processes, with the main dependencies being on the mass ratio of the galaxies, the geometry of the interaction in real space and the projection onto the sky plane (the viewing angle of the observations). In the case of a major merger, however, there is always a clear signal in the higher order coefficients of the Fourier decomposition of the kinemetry (Figure 5). Ram pressure by the intracluster medium, on the other hand, mainly affects the gas disc, pushing away the outer parts and creating distortions at the edge of VFs, while regular rotation can be maintained in the inner regions (Figure 6). In certain configurations, the gas disc can also be displaced from the centre of the stellar disc. During the stripping event, gas can also be compressed so that enhanced star formation is triggered, leading to changes in the stellar populations, too (Kapferer et al., 2009).

In addition, we utilise the simulations to investigate systematically how velocity fields and their characteristic parameters are influenced by the instrumental and observational setup (like spectral resolution, seeing) and for which cases artificial distortions can be induced. A major impact is caused by the decreasing spatial resolution of the spectra when galaxies are observed at higher and higher redshifts. Minor irregularities can be completely smeared out due to seeing and the resolution elements being too coarse.

Currently, we are in the process of analysing each observed galaxy individually. In the case of a regular VF, we perform a TF analysis deriving the rotation curve along the kinematic major axis. For irregular galaxies we examine both the VF and the stellar structure (as revealed on our HST/ACS images) and compare them to a suite of simulated events, taking into account the specific galaxy parameters, in order to pin down the specific interaction mechanism that caused the distortions.

Velocity fields of distant galaxies

The spectroscopic observations using the method presented were performed in Periods 74 and 75 in four different cluster fields (MS1008.1-1224 at $z = 0.30$, MS2137.3-2353 a $z = 0.31$, Cl0412-65 at $z = 0.51$ and MS0451.6-0305 at $z = 0.54$). The target galaxies were not only cluster members but also field galaxies in the background and foreground ($0.1 < z < 0.9$), so that we can investigate different environments. All cluster fields were imaged with ACS onboard HST, enabling an accurate assessment of the morphological structure of the galaxies as well. Our method presented here yielded velocity fields for 49 objects with good signal-to-noise appropriate for our kinemetric analysis. Out of these, there are 16 VFs suitable for investigation of possible interaction processes in rich clusters.

In addition to our detailed analysis with comparison to simulations, we also investigated average properties to assess the abundance of galaxies that have irregular kinematics, irrespective of any assumption of a particular interaction process. To

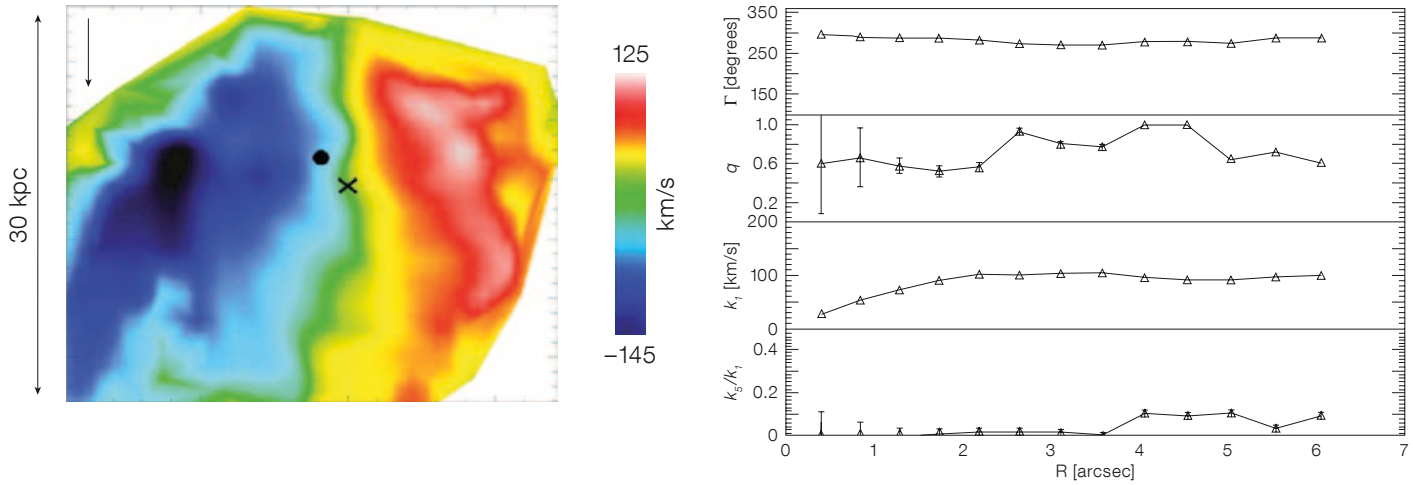

Figure 6. Velocity field of a simulated ram-pressure stripped galaxy as would be observed at $z = 0.1$ and radial profiles (kinematic position angle, flattening, first Fourier coefficient and normalised fifth Fourier coefficient) determined by kinemetry, as in Figure 5a. The case shown refers to one where edge-on ram pressure has already been in action for 400 Myr, with the black arrow indicating intracluster matter wind direction and the cross and circle indicating the kinematic and stellar disc respectively (from Kronberger at al., 2008).

that purpose, we quantify deviations from a simple smooth rotation field with three different indicators measured for each galaxy in the same way. The first two parameters we use are pure gas kinematic tracers: 1) σ_{PA}, the standard deviation of the kinematic position angles of the best-fitting ellipses found by kinemetry across a galaxy; and 2) $k_{3,5}/k_1$, an average value of higher order Fourier coefficients normalised by the rotation velocity. The third parameter compares the global velocity field determined by spectral lines emitted by the (warm) gas content of a galaxy to its morphological structure seen in the continuum light of the stars, given by $\Delta\varphi$, the mean difference between photometric and kinematic position angles across a galaxy. To find an appropriate limit of the value range, below which a galaxy can still be classified as undistorted, we measured the three parameters first for a local sample (taken from Daigle et al., 2006) of 18 gal-

Figure 7. Abundance of galaxies distributed according to our three irregularity parameters, with upper panels: showing the local sample and bottom panels the distant, field (green hashed) and cluster (blue) galaxies. Galaxies are classified irregular if $\Delta\varphi > 25$, $k_{3,5}/k_1 > 0.15$ or $\sigma_{PA} > 20$ degrees (from Kutdemir at al., 2009).

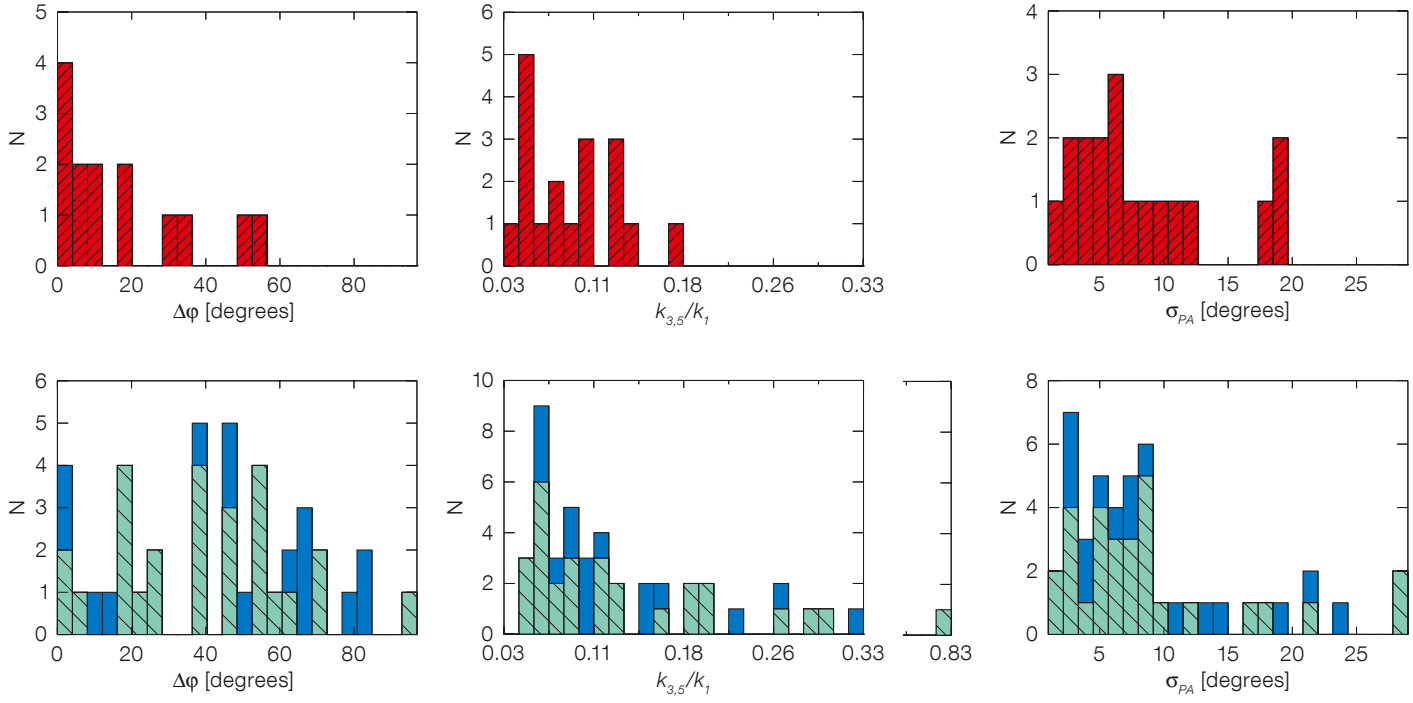

axies that have high resolution VFs (see Kutdemir et al., 2008).

For our distant sample, we find that the fraction of galaxies classified to be irregular according to the three indicators is not unique. For the two pure kinematic tracers we derive a much lower percentage (about 10 % and 30 %) than for the third parameter (about 70 %); see Figure 7 and Kutdemir et al. (2009). The parameters trace different signatures of external processes, but are also sensitive to intrinsic properties. For example, the presence of a bar misaligned with the disc's major axis can also cause a large offset between the gas field and the stellar component. In addition, peculiarities in a VF are more affected by a coarse spatial binning and could be "smeared out". By modelling resolution effects we found that the irregularity fractions we measure are lower limits only.

Furthermore, our simulations show that only strong interactions, like major mergers, induce large values of the kinematic tracers indicating large distortions with high significance. So most of our observed objects with smaller values of the irregularity parameters probably underwent more subtle events. This is presumably also the reason for the surprisingly similar abundance of peculiar galaxies in the field and cluster environment, no matter what indicator is chosen. Since we detect more irregular field galaxies at intermediate redshifts than in the local sample, we are probably witnessing the ongoing growth of their discs via accretion and minor mergers as predicted in CDM models. To clarify decisively the ongoing processes both for field and cluster galaxies, we will, in the near future, examine all available pieces of information for each galaxy (gas VFs, stellar rotation curves, morphologies and stellar populations) and compare them to our simulations.

Acknowledgements

This work was supported financially by Volkswagen-Stiftung (I/76 520), DFG (ZI 663/6), DLR (50OR0602, 50OR0404, 50OR0301) and the Kapteyn institute.

References

Böhm, A. et al. 2004, A&A, 420, 97
Böhm, A. & Ziegler, B. 2007, ApJ, 668, 846
Ferreras, I. et al. 2004, MNRAS, 355, 64
Daigle, O. et al. 2006, MNRAS, 367, 469
Jäger, K. et al. 2004, A&A, 422, 941
Kapferer, W. et al. 2009, A&A, 499, 87
Krajnovic, D. et al. 2006, MNRAS, 366, 787
Kronberger, T. et al. 2007, A&A, 473, 761
Kronberger, T. et al. 2008, A&A, 483, 783
Kutdemir, E. et al. 2008, A&A, 488, 117
Kutdemir, E. et al. 2009, A&A, submitted
Springel, W. 2005, MNRAS, 364, 1105
Tully, R. B. & Fisher, J. R. 1977, A&A, 54, 661
Ziegler, B. et al. 2003, ApJL, 598, 87